TECHNICAL UNIVERSITY OF CLUJ-NAPOCA

ACTA TECHNICA NAPOCENSIS

Series: Applied Mathematics, Mechanics, and Engineering
Vol. 58, Issue III, September, 2015

STUDY OF STRESSES IN TRABECULAR STRUCTURE IN CASE OF FRACTURE TYPE 31-B1.3 USING CANNULATED SCREWS, UNIPODAL SUPPORT

Adrian Ioan BOTEAN

Abstract: *Highlighting the stresses and strain state of trabecular structure in case of proximal epiphysis fracture of the femur (with reference to femoral neck fracture) where, for osteosynthesis, are used cannulated screws, raises multiple technical difficulties. For this reason the present study proposes a synthetic 2D model through which we can identify areas of maximum stress and understanding how the trabecular structure is loaded. The analysis is based on different investigation methods: experimental method using digital image correlation and numerical method using finite element analysis. Mechanical load is specific to unipodal support. For 31-B1.3 fracture type, using Pauwels classification, it was determined that the most dangerous situation is registered when the fracture line is at a 70^o angle to the horizontal line.*

Key words: *human femoral bone, synthetic 2D model, intracapsular fracture, finite element analysis, digital image correlation*

1. INTRODUCTION

Because osteoporosis has no symptoms than when generating a fracture, follows that mode of action of osteoporosis coincides with the expression of fractures that determines. These fractures are overlapping with clinical circumstances that induce the risk of fracture respectively risk factors for osteoporosis, the risk of accidents (the fall, for example) [5].

The fall is defined as "an event that leads a person in involuntary contact with the ground". Are excluded from this category accidents or swoons.

Fractures caused by osteoporosis can be identified through the following characteristics: fractures occur in people with osteoporosis [18]; may occur in female persons after onset of menopause; they are the result of a minor trauma; fractures is localized mainly in the forearm, hip, vertebrae, ribs and less or never in the skull, ankle or fingers [2], [3].

The fracture of the proximal epiphysis of the human femoral bone presents several anatomical types: intracapsular fractures (subcapital fracture or femoral head fracture and transcervical fracture or femoral neck fracture) and extracapsular fractures (intertrochanteric and subtrochanteric). These subtypes of fractures of the proximal femoral epiphysis present different clinical aspects and treated differently.

Femoral neck fracture can provide displacement or angulation of fragments leading to interruption of blood circulation to the femoral head causing avascular osteonecrosis.

There are various classification systems of fractures of femoral neck. Some authors divide femoral fractures in subcapital fracture or femoral head fracture and transcervical fracture or femoral neck fracture. It is noted that the bone structure in the transcervical region is much stronger than in subcapital region so, there is no doubt that in this area there is a higher incidence of fractures. Also, the exact location of the fracture is difficult to determine with radiographs [4], [10], [11], [14].

Common basis of all systems of fractures classification is the size and direction of the displacement.

In this study aims to analyze the state of stresses and strains from 2D models which

presents transcervical fractures and for osteosynthesis are used two rods.

The osteosynthesis 2D model has as the basic element the 2D referential model which presents a trabecular stucture with a number of 170 trabeculae [6], [7]. The area of femoral neck presents a continue fracture line. According to Garden classification this fracture corresponds to the type 2, according to the classification AO/OTA corresponds to the type 31 – B 1.3 and according to Pauwels classification is considered in the three directions of propagation of the fracture line: 30^o, 50^o and 70^o. To fix the distal and proximal area are used two rods positioned at an angle of eight degrees from one another. The two elements are positioned so that the effect of the hull to be as low. Figure 1 shows the positioning of the two rods and defined the three directions of fracture lines according to Pauwels classification.

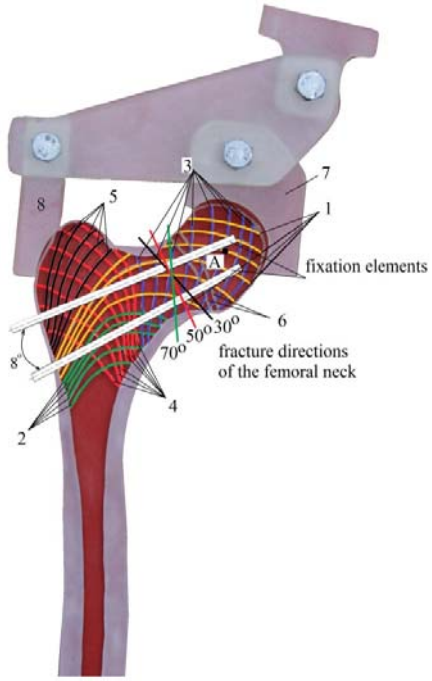

Fig.1 Directions fracture lines according to Pauwels classification: 1 – main tensile group; 2 – secondary tensile group; 3 – main group of compression; 4 – secondary compressions group; 5 – ligamentous group; 6 – growth lines; 7 – hip joint; 8 – small and medium gluteal muscle insertion.

From figure 1 we can see that the two osteosynthesis rods intersect practically most of the elements making up the trabecular structure of proximal femoral bone. The objective of the study is to quantify how it behaves trabecular structure. Such analysis (experimental and numerical) involves the practical realization of three osteosynthesis plane models. Figure 2 presents these 2D models made of epoxy resine and silicone rubber which has three lines of fracture in accordance with Pauwels classification. Experimental, using digital image correlation method, and numerically, using the finite element method, will highlight the state of stresses and strains of trabecular structure, 2D models are mechanical loaded to correspond unipodal support.

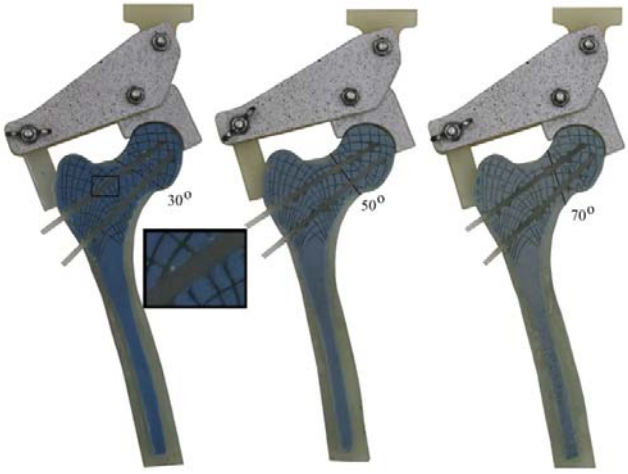

Fig.2 2D models with fracture lines according to Pauwels classification.

2. EXPERIMENTAL ANALYSIS

Mechanic loading system is designed to take into account the hip joint action (femoral head area) and the action of muscles: gluteus medius and gluteus minimus (greater trochanter area). Such a mechanic loading system is properly to unipodal support. In unilateral support or unipodal support hip joint is the point of support for the entire weight of the human body, thus making unilateral support to be the most dangerous position. Here the femoral bone it is stabilized in the acetabulum of muscle group: small, medium and large gluteal muscle.

For charging under load the 2D models shall be used universal testing machine Instron, model 3366, according to figure 3. Mechanical loading is performed static, progressive with forces between 1 to 10 newtons. The load pattern is represented in figure 4. For each

value of the applied force (1, 2, 3, ..., 10 newtons) is defined a constant loading plateau which has a duration of 20 seconds, in which period of time is photographing 2D image model under load.

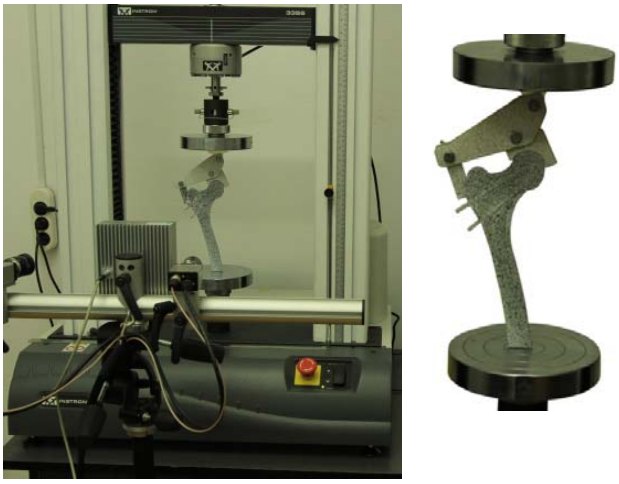

Fig.3 2D model is loaded mechanically through universal testing machine Instron 3366 and analyzed by digital image correlation method with Q400 system.

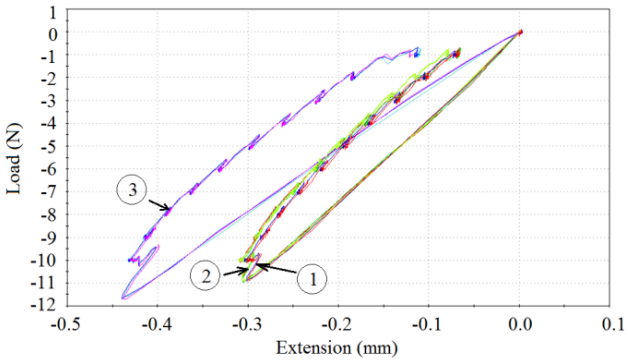

Fig.4 Mechanical load chart for 2D models: 1 – the fracture line at 30°; 2 – the fracture line at 50°; 3 the fracture line at 70°.

Evaluation of the displacement field by using digital image correlation method involves the use of an algorithm which is based on identifying areas of gray. For this reason 2D models surface is painted in white over which is generates a cloud of black dots, as shown in figure 5.

These images are acquired by Q400 system (Dantec Dynamics), the analysis of displacements field being achieved through digital image correlation method using Istra 4D software.

It will assess the displacement, in the vertical plane (dy), of the femoral head center, marked by point A, as shown in figure 1.

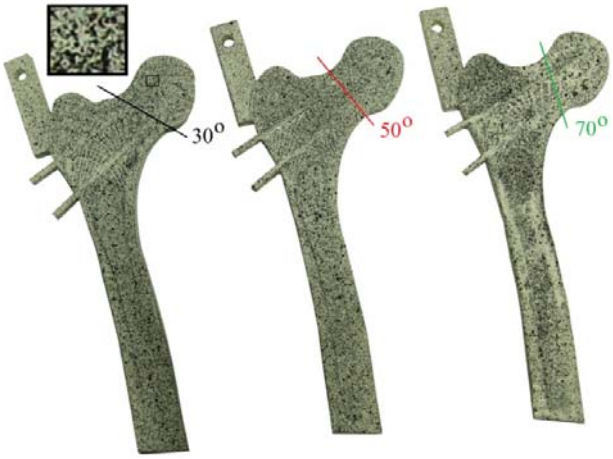

Fig.5 The cloud of black points generated on the surface of 2D models.

Calibration of CCD cameras has a major influence on system performance. Are determined the following parameters: - intrinsec parameters: focal length {x, y}: {2930 ± 120; 2930 ± 120}, principal point {x, y}: {710 ± 40; 520 ± 30}, radial distortion {r^2, r^4}: -0.18 ± 0.05; 0.4 ± 0.9} and tangential distortion {t_x, t_y}: 0.001 ± 0.002; -0.007 ± 0.003}; - extrinsec parameters: rotation vector {x, y, z}: {3.071 ± 0.011; -0.0845 ± 0.0011; 0.24 ± 0.02} and translation vector {x, y, z}: {-38 ± 8; 21 ± 6; 570 ± 20}.

3. NUMERICAL ANALYSIS

2D models are dimensional identical with those made physically, as shown in figure 6. Defining the 2D models is achieved through nodes, in whose positioning shall be used cartesian coordinate system. Numerical modeling implied use of triangular finite elements with six nodes and semicircular sides. Table 1 details the number of nodes and the number of finite elements used for the three 2D models considered.

Numerical, analysis of 2D models is achieved by finite element method using RDM 6.15 software where are defined in cartesian coordinates nodes that allow tracing the contour, it makes meshing and in the distal area of the model is block all degrees of freedom.

Trabecular structure is made by epoxy resine for which longitudinal elastic modulus (Young's modulus) has the value of 2,200 (MPa) and the transverse contractions coefficient has the value of 0.36. The empty spaces of the trabecular structure are filled with silicone rubber for which longitudinal elastic modulus (Young's modulus) has the value of 8 (MPa) and the transverse contractions coefficient has the value of 0.47. Mechanical loading is performed according to the scheme from figure 4. In figure 6 are shown the three 2D numerical models.

Table 1

The modeling characteristics of 2D osteosynthesis models.

Models	Number of nodes	Number of finite elements
30°	14,115	6,874
50°	13,811	6,758
70°	13,646	6,677

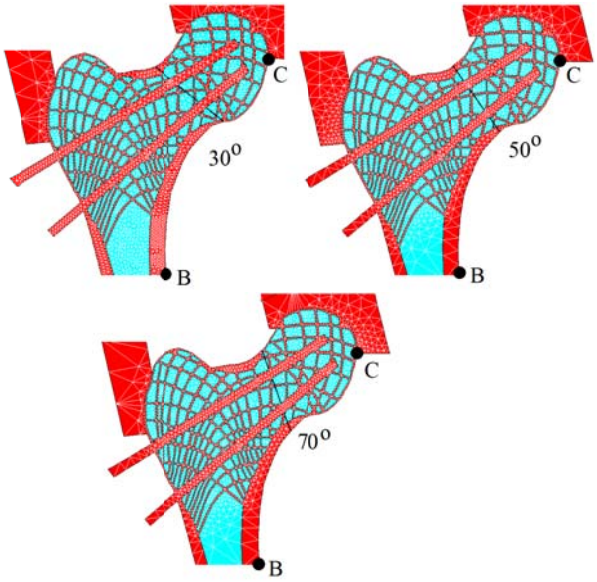

Fig.6 2D numerical models.

4. DISCUSSIONS AND CONCLUSION

2D models can be validated by determining the displacement in vertical plane (dy) of the center of the femoral head (point A in figure 1) both experimental (using digital image correlation method) and numerically (using finite element analysis). In figures 7, 8 and 9 are the values of the displacement in vertical plane (dy) of the point A depending on force P.

Analyzing the results obtained is noted that the average relative deviation in the case of the fracture line which has at 30° it is 4.395 (%) – according to figure 7, for the model which has fracture line at 50° it is 12.135 (%) – according to figure 8 and for the model which has fracture line at 70° it is 12.993 (%) – according to figure 9. In light of these results it can be concluded that the models have a predictable behavior which enables the use of numerical models to assess the state of stresses.

To assess the state of stresses and displacements from trabecular structure is necessary to conduct a comparative analysis of the three 2D models, defined in the figure 6.

The displacement of the center of the femoral head for the three 2D models is assessed through figure 10. In figures 11 and 12 are plotted the variation of stress equivalent Tresca (σ_{Tresca}), the principal stresses σ_1 and σ_2 depending on force P.

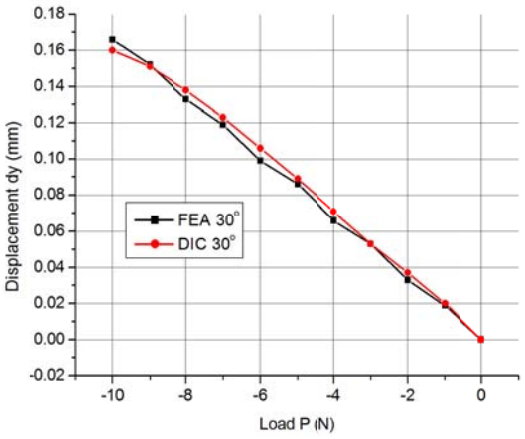

Fig.7 Displacement of the femoral head center depending on load P for 30°.

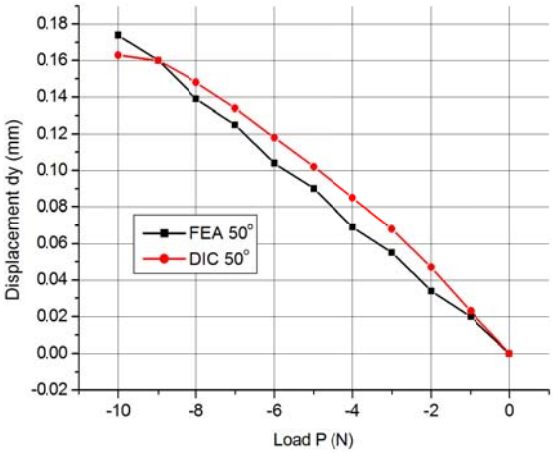

Fig.8 Displacement of the femoral head center

depending on load P for 50°.

From the data presented in the figure 10 may be noted that as the fracture line gradually changes the angle (from 30° to 70°) displacement in vertical plane (dy) of the femoral head center (node A) is progressively increased.

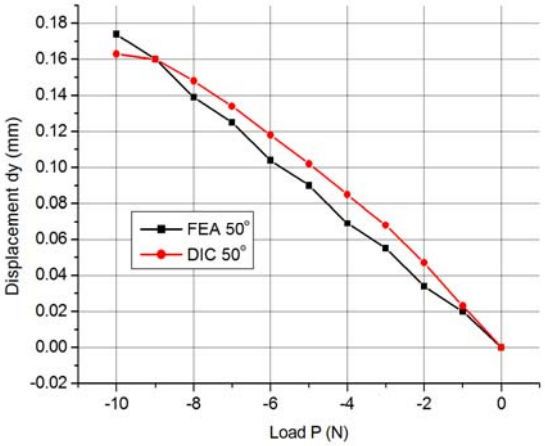

Fig.9 Displacement of the femoral head center depending on load P for 70°.

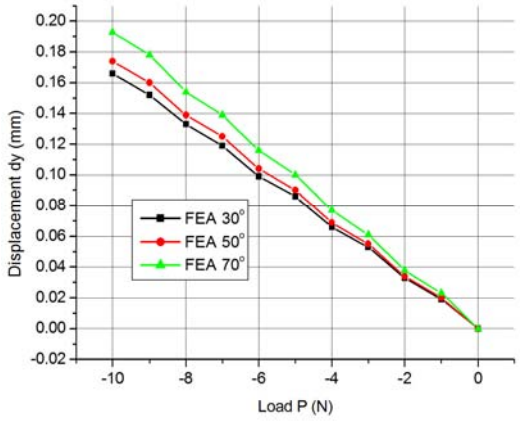

Fig.10 Displacement of the femoral head center depending on the load P for the 3 models considered.

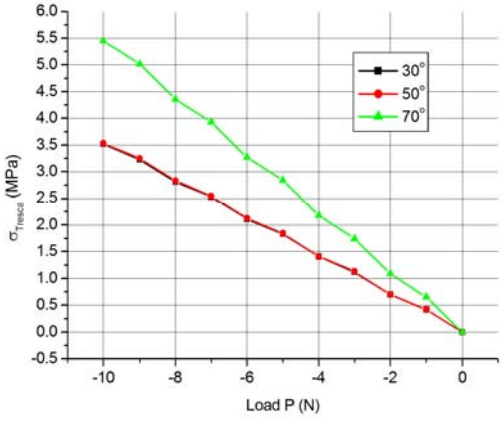

Fig.11 Tresca equivalent stresses variation depending on load P for the 3 models considered.

Thus, if for model in which the fracture line is 30° maximum displacement dy, for the force of 10 (N), is 0.166 (mm), at the model in which the fracture line is 50° displacement dy it is 0.174 (mm) this means an increase of about 4.6% compared to the first model. The model in which the fracture line is 70° displacement dy it is 0.193 (mm) this means an increase of about 14% compared to the first model.

From the data presented in the figure 11 may be noted that as the fracture line gradually changes the angle (from 30° to 70°) a Tresca equivalent stresses (σ_{Tresca}) is gradually increased.

Thus, if for model in which the fracture line is 30° a Tresca equivalent stress, for the force of 10 (N), is 3.52 (MPa), at the model in which the fracture line is 50° a Tresca equivalent stress it is 3.53 (MPa) this means an increase of about 0.3% compared to the first model. The model in which the fracture line is 70° a Tresca equivalent stress it is 5.45 (MPa) this means an increase of about 35.5% compared to the first model.

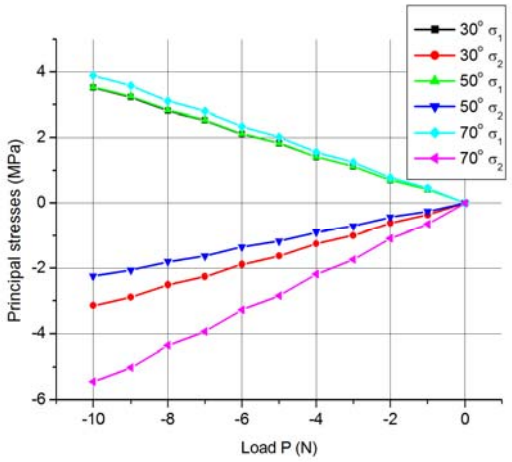

Fig.12 The variation of principal stresses depending on load P for the 3 models considered.

From the data presented in the figure 12 may be noted that as the fracture line gradually changes the angle (from 30° to 70°) a principal tensile stresses (σ_1) is gradually increased. Thus, if for model in which the fracture line is 30° a principal tensile stresses, for the force of 10 (N), is 3.52 (MPa), at the model in which the fracture line is 50° a principal tensile stresses it

is 3.53 (MPa) this means an increase of about 0.3% compared to the first model. The model in which the fracture line is 70° a principal tensile stresses it is 3.89 (MPa) this means an increase of about 9.5% compared to the first model.

In the case of principal compression stresses (σ_2) for model in which the fracture line is 30°, for the force of 10 (N), is 3.14 (MPa), at the model in which the fracture line is 50° is 2.24 (MPa) this means a decrease of about 29% compared to the first model. The model in which the fracture line is 70° a principal compression stresses it is 5.45 (MPa) this means an increase of about 42.5% compared to the first model.

In figure 13 is represented, through the isocolors field, qualitative the distribution of Tresca equivalent stresses (σ_{Tresca}).

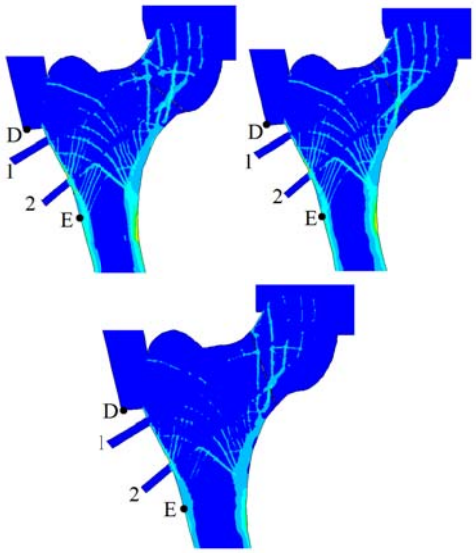

Fig.13 Tresca equivalent stresses distribution in isocolors field.

For quantitative assessment equivalent stresses distribution is plotted of variation thereof (based on analysis of qualitative distribution) on the path defined by the points BC, path highlighted in figure 6, respectively, on the path defined by the points DE, path highlighted in figure 13. Tresca equivalent stresses variation in the case of 2D model where the fracture line is 30° is represented in figures 14 and 15. Tresca equivalent stresses variation in the case of 2D model where the fracture line is 50° is represented in figures 16 and 17. Tresca equivalent stresses variation in the case of 2D model where the fracture line is 70° is represented in figures 18 and 19.

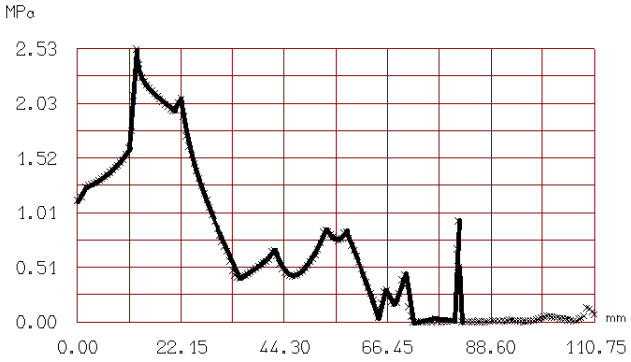

Fig.14 Variation of Tresca equivalent stresses between points BC for 2D model with fracture line at 30°.

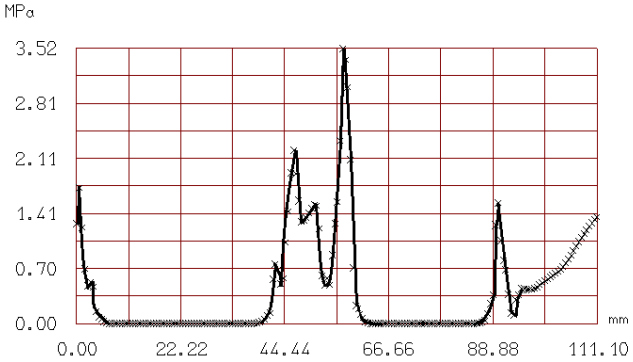

Fig.15 Variation of Tresca equivalent stresses between points DE for 2D model with fracture line at 30°.

The analysis of figures 13, 14 and 15 it appears that on BC path Tresca equivalent stresses registered a maximum value – 2.53 (MPa) – in the area of small trochanter and in the area of fracture line (in inferior fiber of rod 2) has a value of approximately 1 (MPa). On the path between points DE the Tresca equivalent stresses registered a maximum value – 3.52 (MPa) – in the superior fiber of rod 2, also represented the maximum loaded area for the entire 2D model.

In the case of model in which the fracture line is 50°, analyzing figures 13, 16 and 17, is registered the same distribution of Tresca equivalent stresses with the specification that this stresses have higher values. On BC path Tresca equivalent stresses registered a maximum value – 2.24 (MPa) – in the area of small trochanter and in the area of fracture line (in inferior fiber of rod 2) has a value of approximately 1.2 (MPa). On the path between

points DE the Tresca equivalent stresses registered a maximum value – 3.53 (MPa) – in the upper fiber of rod 2, also represented the maximum loaded area for the entire 2D model.

According to figures 13, 18 and 19 for 2D model in which the fracture line is 70°, on the BC path we obtain the same distribution of stresses with the specification that the values are higher in comparison with the first two models. It should be noted that the maximum loaded area in the model migrate from small trochanter area to inferior fiber of rod 2 in the section where the fracture occurs.

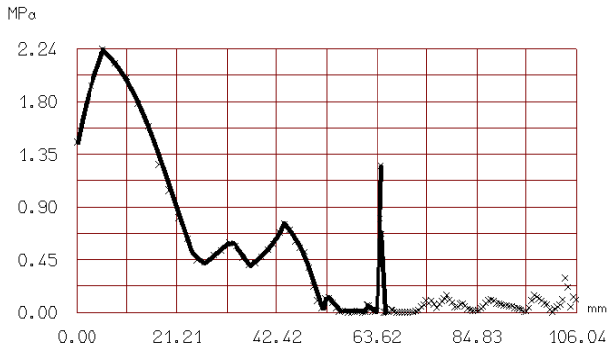

Fig.16 Variation of Tresca equivalent stresses between points BC for 2D model with fracture line at 50°.

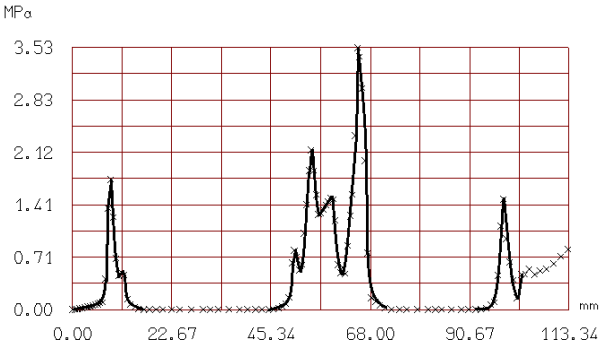

Fig.17 Variation of Tresca equivalent stresses between points DE for 2D model with fracture line at 50°.

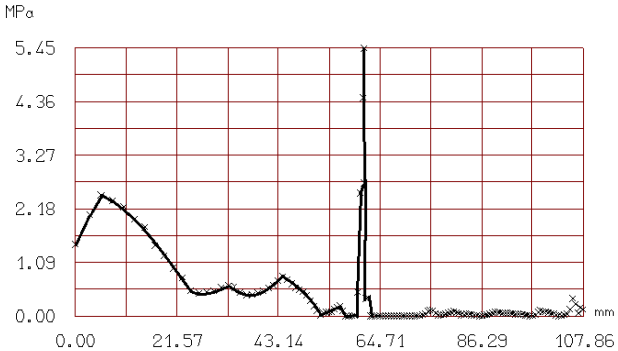

Fig.18 Variation of Tresca equivalent stresses between points BC for 2D model with fracture line at 70°.

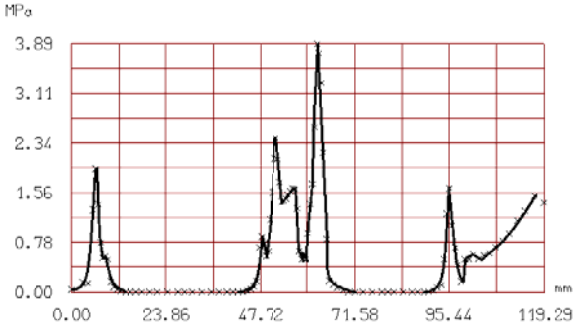

Fig.19 Variation of Tresca equivalent stresses between points DE for 2D model with fracture line at 70°.

It can be concluded that the most dangerous situation is when transcervical fracture, caused by osteoporosis evolution, occurs at a 70° angle to the horizontal line.

5. ACKNOWLEDGEMENTS

This work was possible with the financial support of the Sectorial Operational Programme for Human Resources Development, co-financed by the European Social Found, under the project number PSDRU/159/1.5/S/137516 with the title "Inter-University Partnership for Excellence in Engineering - PARTING".

6. REFERENCES

[1] Ahlborg A.G., Johnell O., Turner C.H. et al., *Bone loss and bone size after menopause*, N Engl J Med, 349:327-334, 2003.

[2] Askin S.R., Bryan R.S., *Femoral neck fractures in young adults*, Clin Orthop, 114:259-264, 1976.

[3] Banks H.H., *Factors influencing the result in fractures of the femoral neck*, J bone Joint Surg Am, 44:931-964, 1962.

[4] Blundell C.M., Parker M.J., Pryor G.A., et al., *Assessment of the AO classification of intracapsular fractures of the proximal femur*, J Bone Join Surg Br, 80(4):679-683, 1998.

[5] Boloşiu H.D., *Osteoporoza*, Casa Cărţii de Ştiinţă, Cluj-Napoca, 2008.

[6] Botean A.I., Mândru D.S., Hărdău M., *Plan model to analyze the state of stresses and strains of the human proximal femoral bone*, Acta Technica Napocensis, Series: Applied Mathematics, Mechanics, and Engineering, Vol.58, II: 199-204, 2015.

[7] Botean A.I., Mândru D.S., Hărdău M., *Modeling human femoral neck using a 2D structure*, Procedia Technology, 19:921-926, 2015.
[8] Bousson V., Meunier A., Bigot C. et al., *Distribution of intracortical bone porosity in human midefemoral cortex by age and gender*, J Bone Miner Res, 16:1308-1317, 2001.
[9] Ettinger M.P., *Aging bone and osteoporosis*, Arch Int Mrd, 163:2237-2246, 2003.
[10] Garden R.S., *Low angle fixation of fractures of the femoral neck*, J Bone Join Surg, 43B:647-663, 1961.
[11] Garden R.S., *Stability and union in subcapital fractures of the femur*, J Bone Joint Surg, 46B:630-647, 1964.
[12] Helfrich M.H., Crockett J.C., Hocking L.J., Coxton F.P., *The pathogenesis of osteoclast disease*, BoneKey Osteovision, 4:61-77, 2007.
[13] Klenerman L., Marcuson R.W., *Intracapsular fractures of the neck of the femur*, J Bone Joint Surg, 52B:514-517, 1970.
[14] Pauwels F., *Der Schenkelhalsbruch: Ein Mechanisches Problem*, Stuttgard: Ferdinand Enke Verlas, 1935.
[15] Parker S., *Corpul uman. Manual complet*, Ediție Litera, 2014.
[16] Riggs B.L., Khosla S., Melton L.J., *A unitary mode of involutional osteoporosis: estrogen deficiency causes both type I and type II osteoporosis in postmenopausal women and contributes to bone loss in ageing men*, J Bone Miner Res, 13:763-773, 1998.
[17] Seeman E., *Structural basis of growth – related gain and age – related loss of bone strenght*, Rheumatol, 47(Suppl 4):2-8, 2007.
[18] Singh M., Nagrath A.R., Maini P.S., *Changes in trabecular pattern of the upper end of the femur as an index of osteoporosis*, The Journal of Bone & Joint Surgery, 52A:457-467, 1970.
[19] Szulcz P., Delmas P.D., *Bone loss in elderly men*, Osteop Int, 18:495-503, 2007.
[20] Tano M., Horiuchi T., Nakajima I. et al., *Age – related changes in cortical and trabecular mineral status*, Acta Radiol, 42:15-19, 2001.
[21] Verken K.V., Bouillon P., Vanderscheuren D., *Androgens versus estrogens: different theories about opposing actions on periosteal bone expansion*, BoneKey, 5:130-136, 2008.
[22] Warming L., Hassager C., Christiansen C., *Changes in bone mineral density with age in men and women*, Osteop Int, 13:105-112, 2002.
[23] ***, *Atlasul corpului uman*, Editura Aquila, 2002.
[24] ***, *Consensus Development Conference on Osteoporosis, Osteoporosis Prevention, Diagnosis, and Therapy*, The Journal of the American Medical Association, 285: 785-795, 2001.
[25] ***, *Rockwood and Green's, Fractures in Adults*, Vol.2, 8 Edition, Wolters Kluwer, 2015.

Studiul tensiunii din structura trabeculară in cazul fracturii de tip 31-B1.3 utilizând şuruburi canulate, sprijin unipodal

Rezumat: *Evidențierea stării de tensiuni şi deformații din structura trabeculară în cazul fracturii epifizei proximale a femurului (cu referire la fractura colului femural) atunci când, pentru osteosinteză, sunt utilizate şuruburi canulate ridică multiple dificultăți de ordin tehnic. Din acest motiv prin prezentul studiu se propune un model 2D sintetic prin intermediul căruia se pot identifica zonele de maximă solicitare precum şi înțelegerea modului în care structura trabeculară este solicitată. Analiza are la bază metode de investigare experimentale (corelația digitală a imaginii) şi numerice (metoda elementului finit). Solicitarea mecanică este specifică sprijinului unipodal. Pentru fractura de tip 31-B1.3, utilizând clasificarea Pauwels, s-a stabilit faptul că cea mai periculoasă situație se înregistrează când linia de fractură este la un unghi de 70^o în raport cu orizontala.*

Adrian Ioan BOTEAN, Lecturer, Ph.D., Technical University of Cluj-Napoca, Department of Mechanical Engineering, 103-105 Muncii Blvd., 400641, Cluj-Napoca, +40-264-401751, Adrian.Ioan.Botean@rezi.utcluj.ro.